Bulletin of Electrical Engineering and Informatics
Vol. 14, No. 2, April 2025, pp. 1138~1150
ISSN: 2302-9285, DOI: 10.11591/eei.v14i2.7833

Machine learning-based and synthetic aperture radar time-series data for rice classification over Sentinel-1 imagery

Attawut Nardkulpat[1], Wuttichai Boonpook[1], Asamaporn Sitthi[1], Yumin Tan[2]
[1]Department of Geography, Faculty of Social Sciences, Srinakharinwirot University, Bangkok, Thailand
[2]School of Transportation Science and Engineering, Beihang University, Beijing, China

Article Info

Article history:

Received Nov 5, 2023
Revised Oct 21, 2024
Accepted Nov 19, 2024

Keywords:

Machine learning
Rice classification
Sentinel-1 time series data
Suphan buri
Synthetic aperture radar

ABSTRACT

Rice extraction is critical in remote sensing, especially in Suphan Buri province, Thailand, using Sentinel-1 synthetic aperture radar (SAR) time-series data and advanced machine learning algorithms. Given the challenges of varied terrains and diverse crop types, the research employs different polarization modes (vertical transmit and vertical receive (VV), vertical transmit and horizontal receive (VH), and VV+VH) to enhance classification accuracy. The study evaluates the performance of three machine learning algorithms: random forest, extreme gradient boosting (XGBoost), and light gradient boosting machine (LightGBM). The results demonstrate that combined VV+VH polarization outperforms VV and VH alone, providing better accuracy due to its ability to capture more detailed object features. LightGBM emerged as the most effective among the algorithms, particularly when dealing with large datasets. After hyperparameter tuning (n_estimators: 820, max_depth: 10, and learning_rate: 0.01), LightGBM achieved the highest accuracy. The rice class showed exceptional precision, recall, and F1-score, surpassing other land-use classes (agriculture/forest and urban areas). However, these classes still pose challenges, highlighting the need for future studies to integrate multi-sensor data and explore more sophisticated machine-learning models. This research offers a promising approach to enhancing rice monitoring and management in diverse agricultural landscapes, contributing to more accurate and efficient farming practices.

Corresponding Author:

Wuttichai Boonpook
Department of Geography, Faculty of Social Sciences, Srinakharinwirot University
Bangkok, Thailand
Email: wuttichaib@g.swu.ac.th

1. INTRODUCTION

Rice is one of the world's most important cereal crops and a staple food for a significant portion of the global population, particularly in Asia. In 2020–2021, Thailand ranked as the world's top rice producer and exporter, accounting for second in global output [1]. Thailand grows most of its rice in the northeastern, lower northern, and central regions, spanning 68.86 million hectares [2]. To cultivate and assess various aspects of rice production, remote sensing imagery serves as a valuable tool for rice identification and mapping, rice health assessment, yield estimation, monitoring growth stages, disease, and pest detection [3].

Remote sensing technology plays a key role in rice monitoring and management. Ground surveys and remote sensing techniques source this invaluable information. The currency and precision of this data are pivotal for various land use applications. While ground surveys offer exceptional accuracy, they often require more time and financial resources [4]. In contrast, remote sensing methods provide up-to-date information

and extensive coverage, making them a practical choice for many applications. Satellite imagery is the primary data source for remote sensing. There are two primary types of sensors used for data collection: passive and active sensors. The Earth's surface emits or reflects electromagnetic radiation, which a passive sensor detects and records. This sensor provides multispectral bands that are suitable for rice classification. However, the sensors rely on available sunlight or natural radiation sources for data collection [5]. On the other hand, an active sensor emits electromagnetic radiation towards the Earth's surface. This emitted energy interacts with objects on Earth's surface, and the sensor records the reflected energy. The sensor transmits and receives signal polarization both vertically and horizontally, which limits feature dimensions [6]. Nonetheless, the advantage of active sensors is their ability to operate day and night, regardless of atmospheric conditions such as clouds, rain, or fog. Their resilience to adverse weather conditions sets them apart from passive sensors. Synthetic aperture radar (SAR) is an active sensor technology that can operate day and night, regardless of atmospheric conditions, making it particularly useful for agricultural monitoring.

SAR technology has proven effective in rice field detection and monitoring. Numerous studies have been conducted to investigate the use of SAR data for discerning rice fields. Several of these studies have demonstrated the efficacy of SAR data across various frequency bands including X-band [7] and C-band [8] for monitoring rice [9]. Sentinel-1A imagery, a SAR product, has been utilized for detecting rice distribution through the analysis of Sentinel-1A time series data [10]. It explored temporal fluctuations in backscatter coefficients throughout the rice growing cycle. During the sowing stage, paddy fields are typically inundated with water, resulting in a decrease in backscatter due to specular reflection. As the rice matures, there is an observed increase in backscatter due to the limited penetration of active sensors in the rice plants. The temporal backscattering coefficient of rice exhibits its lowest value during the agronomic flooding phase, followed by an increase during the tillering stage. Subsequently, the backscatter coefficient experiences a decline. The use of radar reflection for rice crop analysis has been found to display a significant range of variability throughout the growth cycle [11]. In response to this variability, Chen [12] introduced the concept of the normalized difference sigma-naught index (NDSI), which was derived from time-series data of Sentinel-1A vertical transmit and horizontal receive (VH) and vertical transmit and vertical receive (VV) polarizations. The NDSI, representing the backscatter difference between the maximum and minimum values in the time-series data, was employed to map rice fields. The results of this approach showed an impressive overall accuracy of 92.1% and a kappa coefficient of 0.85 specifically for VH polarization. Furthermore, Mansaray *et al.* [13] established a backscatter variation threshold to enhance the mapping of paddy rice. The threshold was determined through an analysis of the spatial dynamics of rice backscattering, driven by variations in flooding, tillering, and booting across diverse fields. This approach yielded a classification accuracy of 88.3% and a kappa coefficient of 0.85. Nguyen and Wagner [14] conducted a validation study to evaluate the effectiveness of a phenology-based categorization approach for mapping rice fields across a continental scale. This categorization methodology relied on three critical factors: the maximum backscatter value, the difference between the maximum backscatter and the backscatter recorded at the start of the growth season, and the temporal duration between the initial date and the date of maximum backscatter. The results of the study indicated that the overall accuracy exceeded 70% for all the areas investigated [15]. Furthermore, an analysis of the temporal dynamics of the SAR backscattering coefficient of rice, their research introduced three matrices derived from the analysis of the Gaussian profile of the VV/VH time-series, the variance of the VV/VH time-series, and the slope of the linear regression of the VH time-series. These matrices were employed for mapping rice plots using decision trees and random forest classifiers. The results demonstrated a remarkable level of accuracy, with the decision tree classifier achieving an overall accuracy of 96.3%, and the random forest classifier achieving an even higher accuracy of 96.6% [16].

The integration of remote sensing technologies with machine learning algorithms is leading to significant progress in multiple areas of environmental and Earth system studies [17]. Machine learning enables researchers to discover intricate patterns and connections within this data, revealing crucial insights that were previously challenging or unattainable. This collaboration allows for more precise identification and categorization of land cover [18], improved agricultural practices [19], enhanced monitoring and evaluation of disasters [20], analysis of climate change impacts [21], and better urban planning [22]. Machine learning approaches, such as deep learning, are highly proficient at identifying patterns in large amounts of remote sensing data. This allows for the automated extraction of valuable information, a process that is frequently too difficult for traditional analysis methods [23]. However, light gradient boosting (LightGBM), an advanced gradient-boosting machine framework, is revolutionizing the field of machine learning. LightGBM was created to overcome the constraints of previous models by utilizing advanced techniques like as gradient-based one-side sampling (GOSS) and exclusive feature bundling (EFB). These techniques significantly enhance the speed of training and the efficiency of memory usage, while maintaining high predicted accuracy. This feature makes it a perfect option for managing extensive, multi-dimensional datasets that are becoming more and more common in contemporary applications. LightGBM's leaf-wise tree growth technique significantly improves its performance, frequently attaining comparable or superior results

compared to other prominent gradient-boosting algorithms [24]. LightGBM surpasses traditional machine learning models such as support vector machines, random forests, and artificial neural networks. Its exceptional speed and efficiency enable it to handle the extensive datasets produced by time-series SAR, while its robustness in managing noisy and potentially incomplete data ensures precise rice area identification. Compared to traditional models, LightGBM exhibits superior performance in capturing subtle temporal variations in SAR backscatter, a critical factor for distinguishing rice crops from other land cover types. By leveraging the combined strengths of LightGBM and time-series SAR data, the classification results achieve greater accuracy and precision in identifying rice areas, ultimately facilitating more effective monitoring, management, and decision-making in agricultural applications [25]. The objective of this research is to utilize Sentinel-1 time series SAR data and machine learning methods, including LightGBM, extreme gradient boosting (XGBoost), and random forest, to classify various rice cultivation areas in central Thailand. This research expands upon prior studies that utilized SAR data to monitor rice crops. and aim to utilize the distinctive benefits of ensemble techniques with LightGBM, XGBoost, and random forest for effective and precise classification of time-series datasets that encompass various.

2. STUDY AREA AND DATA COLLECTION

2.1. Study area

Suphan Buri Province, located in central Thailand as shown in Figure 1(a), exhibits a varied pattern of land use due to its diverse landscape, agricultural activities, and economic development. Approximately 72.44% of the province's land is designated for agricultural purposes. Notably, it is known for the cultivation of major crops, including rice, sugarcane, cassava, and maize, as well as fruits like oranges and longan. Rice fields encompass an area of approximately 1,992 square kilometers, constituting about 37.18% of the province's total land area [26]. Both in-season and off-season rice cultivation practices are prevalent in this province. In-season rice is planted during the wet or monsoon season. The main planting season usually begins in May to July and continues into the rainy season, which typically lasts until October. Off-season rice is planted in the dry season, typically from November to February. These crops rely on irrigation systems, as natural rainfall is limited during this time. Rice in Suphan Buri is typically harvested a few months after planting, depending on the variety and growing conditions [27]. Temperature, rainfall, and irrigation system are critical environmental factors that significantly influence rice planting and cultivation in Suphan Buri province.

Indeed, the presence of various planting stages in Suphan Buri Province as shown in Figure 1(b), occurring from May to July and with harvests typically taking place from September to November, can introduce challenges for rice classification using SAR imagery. The shifting crop calendar leads to the simultaneous presence of multiple rice growth stages, as depicted in Figure 1(c), complicating the differentiation and accurate classification of rice fields. Therefore, accounting for these variating and developing robust classification methods are important considerations in rice monitoring and management in the region.

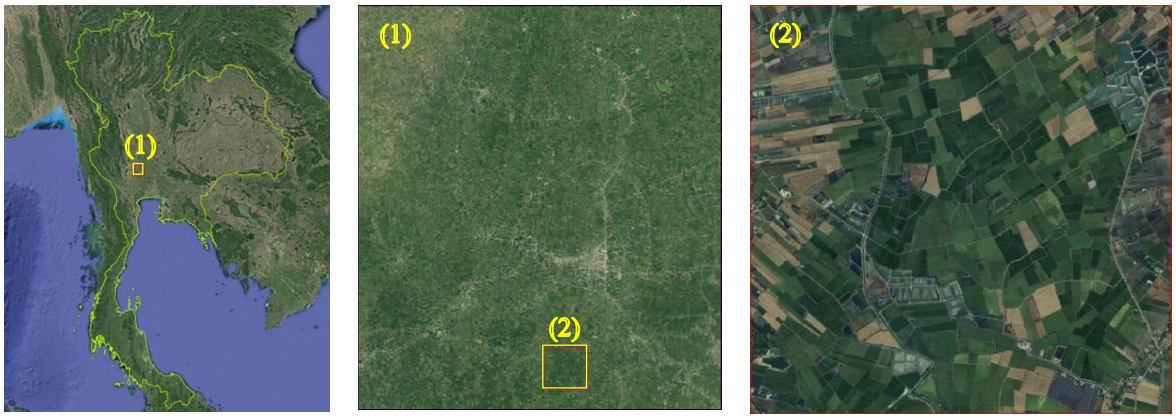

(a) (b) (c)

Figure 1. Study area location in Thailand: (a) map showing the national boundary of Thailand, (b) map indicating the specific location of the study area, and (c) rice fields cultivated during different periods

2.2. Sentinel-1 time series data

Sentinel-1 is equipped with (SAR) instruments that can capture images of the Earth's surface day and night. The dual-polarized interferometric wide swath (IW) provides VV and VH. Sentinel-1 generally covers paths from 23 to 146 and rows from 1 to 418. Suphan Buri province is in path 62 and row 15. The Sentinel-1 data used in this research was captured from January 2022 to December 2022. The data obtained is ground range detection (GRD) image data in the C-band wave range with the length of the range. A polarization waveform characterizes the 5.405 GHz wave in the descending satellite trajectory, taking the same orbital repeating time at most 12 days. Image resolution in range and azimuth is 5×20 meters (provided by the spatial resolution of 10×10 meters) [28] as detailed in Table 1.

Table 1. Sentinel-1 data acquisition

Sensor	SAR C-band
Product level	Level 1 GRD
Data acquisition (yyyy-mm-dd)	2022-01-12; 2022-01-24; 2022-02-05; 2022-02-17; 2022-03-13; 2022-03-25; 2022-04-06; 2022-04-18; 2022-04-30; 2022-05-12; 2022-05-24; 2022-06-05; 2022-06-17; 2022-06-29; 2022-07-11; 2022-07-23; 2022-08-04; 2022-08-16; 2022-08-28; 2022-09-09; 2022-09-21; 2022-10-03; 2022-10-27; 2022-11-08; 2022-11-20; 2022-12-02; 2022-12-14; 2022-12-26
Frequency (GHz)	5.405
Image mode	IW
Polarization	VH+VV

3. METHOD

3.1. Preprocessing data

For the preprocessing of Sentinel-1 data, Google Earth Engine (GEE) was employed to enhance the quality and usability of radar imagery. This involved a series of sequential steps, including orbit correction, removal of GRD border noise, thermal noise removal, radiometric calibration, conversion to decibels (dB), terrain correction, speckle filtering, and log scale conversion [29]. In total, 28 images from the Sentinel-1 time-series dataset were utilized. The training, validating, and testing datasets were sourced from land use and land cover data provided by the Land Development Department, Ministry of Agriculture and Cooperatives, Thailand. These datasets were obtained through random sampling of 6,938 points, ensuring an even distribution across the study area categorized into four classes: agriculture and forest, rice, urban, and water as shown in Figure 2. The summary of the temporal profile of four land use categories, Figures 3(a) and (b) shows the monthly average backscatter coefficient of a sample in different land use categories for VV polarization and VH polarization, respectively, categorized by polarization.

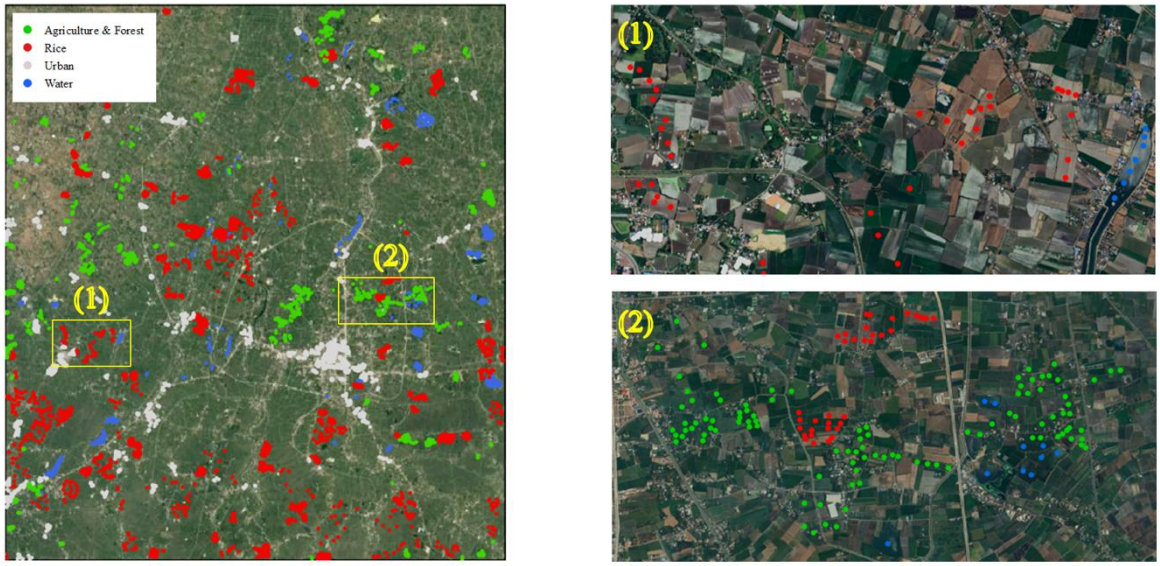

Figure 2. Spatial distribution of training data points in agriculture/forest class, rice class, urban class, and water class

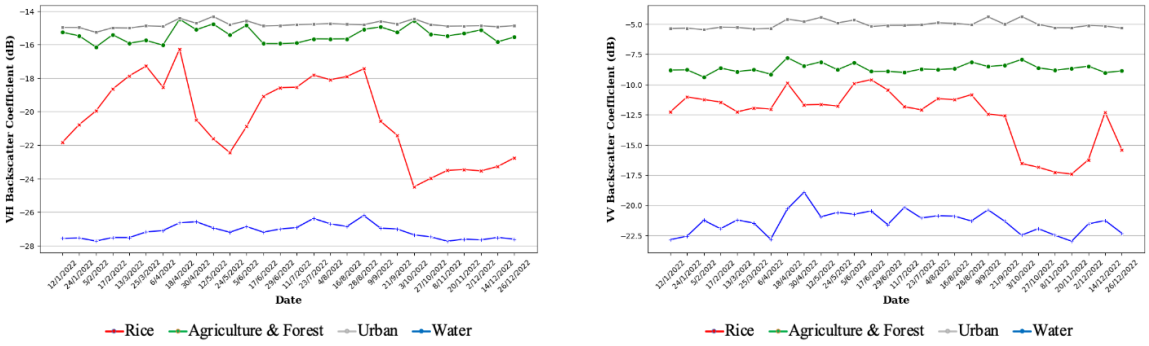

(a) (b)

Figure 3. Temporal profiles of the four different land use types with respect: (a) VH and (b) VV average backscatter coefficient (dB)

3.2. Machine classifier

Machine learning classification algorithms are highly versatile and can be effectively applied to a wide spectrum of remote sensing classification tasks. The selection of the most suitable algorithm is contingent upon factors such as the unique characteristics of the problem, the size, and quality of the dataset, as well as the interpretability and computational demands of the model. Considering this, the present study carefully chooses the most appropriate classification algorithm that aligns with the specific characteristics and data features of the problem. Three distinct classification algorithms, namely random forest, XGBoost, and LightGBM, were employed for the analysis of Sentinel-1 time series data, encompassing various polarizations. The random forest algorithm was initially proposed by Breiman [30] as a method for constructing an ensemble of learning tree classifiers. The primary concept of the approach involves extracting the values of a randomly generated vector from a combined bootstrap sample, specifically the training dataset. Subsequently, several decision trees are trained using these values. Nevertheless, the trained decision tree model may generate a substantial number of trees.

One of the primary benefits of XGBoost is its ability to parallelize computations. XGBoost, a variant of the gradient boosting machine technique, has demonstrated scalability and efficiency across various machine learning applications. Chen and Guestrin [31], XGBoost is a machine learning algorithm that combines several classification and regression trees to handle datasets including nonlinear features. The primary concept involves the utilization of weak trees and the improvement of tree accuracy with each iteration. This approach considers the prediction error from the previous outcome of a weak tree. It subsequently trains the next tree classifier to incorporate the mistake of the already trained ensemble. The LightGBM framework, which is relatively recent, finds extensive usage in several machine learning and data science domains. One of the primary concerns associated with gradient boosting algorithms is the comprehensive processing of all data in order to determine potential separation points, which can have a significant impact on performance. The optimal search methodology has been enhanced through modifications in this method [24].

3.3. Model training and tuning

In this study, the dataset obtained from the Land Development Department for the year 2022 was utilized. The dataset was randomly partitioned into three subsets: a training set including 60% of the data, a validating set also accounting for 20% of the data, and a testing set consisting of 20% of the data. Feature extraction from time-series SAR data involves analyzing the backscattered signal's temporal variations. Key features include the temporal backscatter intensity values at each pixel, indicating the amount of radar energy reflected over time. The grid search approach was employed to ascertain the optimal values for the model parameters, including the learning rate, tree depth, and subsampling rate. The grid search method is employed to assess the efficacy of various parameter combinations on a given dataset through the utilization of cross-validation. The best parameter combination is determined by selecting the parameter value that yields the highest evaluation metric. The parameter ranges chosen for the grid search are presented in Table 2.

The technique of K-fold cross-validation was employed to determine the optimal hyperparameter. The approach can achieve outcomes that are 0.1-3% more accurate than the hold-out method, which involves conducting training and validation only once. The process of K-fold cross-validation involves partitioning the training and validation datasets into K subsets. During each iteration, one subset is used as the validation data while the remaining K-1 subsets are used for model training. This process is repeated K times, the hyperparameter accuracy was determined by calculating the average accuracy of the training and validating

datasets, which were separated into K subsets. The hyperparameter with the highest average accuracy was chosen as the optimal hyperparameter.

Table 2. Hyperparameter search range

Classifier	Hyperparameter	Search range
Random forest	n_estimators	100–1,000
	max_depth	10–120
	min_samples_split	7, 13, 20
XGBoost	n_estimators	100–1,000
	max_depth	2, 4, 6, 8, 10
	learning_rate	0.01, 0.05, 0.1
LightGBM	n_estimators	100–1,000
	max_depth	2, 4, 6, 8, 10
	learning_rate	0.01, 0.05, 0.1

3.4. Accuracy assessment

To evaluate the multi-class classification from machine learning algorithms, this research applied overall accuracy, Kappa coefficient, precision, recall, and F1-score. In remote sensing image multi-class classification, several evaluation metrics can be used to assess the performance of a model. One of the most common ways to evaluate a multi-class classification model is through a confusion matrix. A confusion matrix is a table used to evaluate a classification model's performance. The table shows the number of true positives (TP), false positives (FP), true negatives (TN), and false negatives (FN) for each class in the classification problem [31]. The confusion matrix can be represented as follows:

The overall accuracy is the proportion of correctly classified instances over the total number of instances. Mathematically, it can be expressed as (1):

$$\mathrm{OA} = \frac{\sum_{i=1}^{n} c_{ii}}{\sum_{i=1}^{n} \sum_{j=1}^{n} c_{ij}} \quad (1)$$

where c_{ii} is the number of correctly classified instances for class i and n is the number of classes.

On the other hand, the Kappa coefficient [32] considers the possibility of correct classification by chance. It is defined as the difference between the observed and expected accuracy, normalized by the maximum possible difference. Mathematically, it can be expressed as (2):

$$\widehat{K} = \frac{N \sum_{i=1}^{r} X_{ii} - \sum_{i=1}^{r} X_{i+} X_{+i}}{N^2 - \sum_{i=1}^{r} X_{i+} X_{+i}} \quad (2)$$

where r represents the number of rows and columns in the error matrix, N is the total number of observations, X_{ii} is the observation in row i and column i, X_{i+} is marginal total of row i, and X_{+i} is the marginal total of column i.

Precision, recall, and F1-score [33] are metrics that evaluate the performance of a classifier for each class. Precision is the proportion of true positives among all predicted positives, recall is the proportion of true positives among all actual positives, and F1-score is the harmonic mean of precision and recall. They can be calculated as (3)-(5):

$$\mathrm{Precision}_i = \frac{\mathrm{TP}_i}{\mathrm{TP}_i + \mathrm{FP}_i} \quad (3)$$

$$\mathrm{Recall}_i = \frac{\mathrm{TP}_i}{\mathrm{TP}_i + \mathrm{FN}_i} \quad (4)$$

$$\mathrm{F1\ score}_i = 2 \frac{\mathrm{Precision}_i \times \mathrm{Recall}_i}{\mathrm{Precision}_i + \mathrm{Recall}_i} \quad (5)$$

where i represents each class, these metrics can be used to evaluate the performance of a multi-class classification model.

4. RESULTS

In this result section, we design two experiments to evaluate the performance of the machine learning algorithm and Sentinel-1 time-series data for rice classification. The first experiment illustrates the best fine-tuning hyperparameters for machine learning algorithms (random forest, XGBoost, and LightGBM)

and the different data polarizations (VV, VH, and VV+VH). The second experiment evaluates the performance of machine learning algorithms for rice classification.

4.1. The performance of fine-tuning hyperparameters for machine learning algorithms and the different time-series data polarizations

As shown in Table 3, the comparison of each machine learning algorithm and the different time-series data polarizations show that the LightGBM algorithm outperforms XGBoost and random forest algorithms and the combination of VV and VH polarizations overcomes the time-series VV polarization and time-series VH polarization as shown with the highest overall accuracy and Kappa coefficient. LightGBM algorithm and the time-series VV+VH polarization with hyperparameters setting (n_estimators, max_depth, and learning rate were defined optimal values as 820, 10, 0.01, respectively) present the highest performance with 91.64% of overall accuracy and 0.88 of Kappa coefficient. Its performance overcomes the XGBoost algorithm with hyperparameters setting around 0.16% of overall accuracy and the same value of Kappa coefficient, and the Random Forest algorithm with hyperparameters setting around 1.65% of overall accuracy and 0.02 of Kappa coefficient. Moreover, in the LightGBM algorithm, the time-series VV+VH polarization data shows better overall accuracy at 91.64% which overcomes the time-series VV polarization at around 2.53% of overall accuracy and the time-series VH polarization with 6.18% of overall accuracy. Compared to other machine learning algorithms, in XGBoost, the time-series VV+VH polarization data also outperforms overall accuracy with 91.48% higher than the time-series VV polarization around 2.72% and time-series VH polarization around 7.13%, respectively. In the random forest algorithm, the time-series VV+VH polarization data also outperforms overall accuracy with 89.99% higher than the time-series VV polarization around 2.03%, and time-series VH polarization around 5.27%, accordingly.

Table 3. Hyperparameter selection according to the optimization method by different algorithms

Classifier	Dataset	Hyperparameter	Optimal value	each	Kappa coefficient
Random forest	VV	n_estimators	520	87.96	0.83
		max_depth	34		
		min_samples_split	7		
	VH	n_estimators	340	84.72	0.79
		max_depth	71		
		min_samples_split	7		
	VV+VH	n_estimators	290	89.99	0.86
		max_depth	71		
		min_samples_split	7		
XGBoost	VV	n_estimators	570	88.76	0.84
		max_depth	6		
		learning_rate	0.05		
	VH	n_estimators	970	84.35	0.78
		max_depth	8		
		learning_rate	0.1		
	VV+VH	n_estimators	510	91.48	0.88
		max_depth	4		
		learning_rate	0.05		
LightGBM	VV	n_estimators	440	89.11	0.85
		max_depth	10		
		learning_rate	0.05		
	VH	n_estimators	290	85.46	0.80
		max_depth	10		
		learning_rate	0.05		
	VV+VH	n_estimators	820	91.64	0.88
		max_depth	10		
		learning_rate	0.01		

4.2. The effectiveness of classification algorithms and sentinel-1 time-series data polarizations for rice classification

Table 4 presents each class's classification results, which are evaluated by precision, recall, and F1-score. As explained in the performance of machine learning algorithms and sentinel-1 time-series data polarization in subsection 3.1, the LightGBM algorithm and time-series VV+VH polarization show the best performance in overall accuracy and kappa coefficients. The classification results for each class also demonstrate the accuracy and effectiveness of the classification process for each land use class. In the agriculture/forest class, a precision score of 0.91, a recall rate of 0.80, and an F1-score of 0.85 were achieved. Within the urban class, precision stood at 0.79, and recall reached an impressive 0.92, resulting in an F1-score of 0.85. The water class demonstrated a precision of 0.99, a recall of 0.98, and an F1-score of 0.99.

Notably, the rice class exhibited exceptional metrics, boasting a precision of 0.97, a recall rate of 0.96, and an exceptional F1-score of 0.97. When employing the XGBoost algorithm and time-series VV+VH polarization, the agriculture/forest class yielded a precision of 0.89, a recall rate of 0.81, and an F1-score of 0.85. The rice class achieved a precision score of 0.97, a recall of 0.96, and an F1-score of 0.97. For the urban class, precision reached 0.81, and recall stood at 0.90, resulting in an F1-score of 0.85. The water class, once again, delivered impressive results with a precision of 0.99, a recall rate of 0.99, and an outstanding F1-score of 0.99. Within the framework of the random forest algorithm and time-series VV+VH polarization, the agriculture/forest class secured a precision score of 0.90, a recall rate of 0.80, and an F1-score of 0.85. The rice class showcased a precision of 0.98, a recall rate of 0.92, and an F1-score of 0.95. In the urban class, precision was recorded at 0.72, and recall reached 0.93, resulting in an F1-score of 0.81. The water class excelled with a precision of 0.99, a recall rate of 0.98, and an F1-score of 0.99. As for the LightGBM algorithm and time-series VV polarization, there is a noticeable decrease in performance when compared to VV+VH polarization.

Table 4. The accuracy result of rice classification is based on the following algorithms and datasets

Dataset	Classifier	Class	Precision	Recall	F1-score
VH	Random forest	Agriculture/forest	0.76	0.70	0.73
		Rice	0.98	0.93	0.95
		Urban	0.64	0.77	0.70
		Water	0.99	0.97	0.98
	XGBoost	Agriculture/forest	0.73	0.68	0.71
		Rice	0.96	0.95	0.96
		Urban	0.68	0.75	0.71
		Water	0.98	0.97	0.97
	LightGBM	Agriculture/forest	0.75	0.69	0.72
		Rice	0.97	0.96	0.97
		Urban	0.70	0.77	0.73
		Water	0.98	0.98	0.98
VV	Random forest	Agriculture/forest	0.86	0.75	0.80
		Rice	0.98	0.90	0.94
		Urban	0.69	0.93	0.79
		Water	0.99	0.99	0.99
	XGBoost	Agriculture/forest	0.85	0.74	0.80
		Rice	0.97	0.94	0.95
		Urban	0.74	0.89	0.81
		Water	0.98	0.99	0.99
	LightGBM	Agriculture/forest	0.86	0.75	0.80
		Rice	0.97	0.95	0.96
		Urban	0.76	0.89	0.82
		Water	0.98	0.99	0.98
VH+VV	Random forest	Agriculture/forest	0.90	0.80	0.85
		Rice	0.98	0.92	0.95
		Urban	0.72	0.93	0.81
		Water	0.99	0.98	0.99
	XGBoost	Agriculture/forest	0.89	0.81	0.85
		Rice	0.97	0.96	0.97
		Urban	0.81	0.90	0.85
		Water	0.99	0.99	0.99
	LightGBM	Agriculture/forest	0.91	0.80	0.85
		Rice	0.97	0.96	0.97
		Urban	0.79	0.92	0.85
		Water	0.99	0.98	0.99

The agriculture/forest class demonstrates good precision at 0.86, with a recall of 0.75, resulting in an F1-score of 0.80. The rice class, however, maintains its impressive performance, boasting a precision of 0.97, a recall of 0.95, and an F1-score of 0.96, indicating robust classification capabilities. In the urban class, precision is 0.76, with a recall of 0.89, leading to an F1-score of 0.82. The water class continues to excel, achieving a precision of 0.98, a recall of 0.99, and an F1-score of 0.98, reaffirming its outstanding classification prowess.

The LightGBM algorithm, when coupled with time-series VH polarization, demonstrates a slightly lower performance compared to time-series VV polarization and VV+VH polarization. In the agriculture/forest class, precision is measured at 0.75, with a recall of 0.69, resulting in an F1-score of 0.72. The rice class continues to excel with a precision of 0.97 and a recall of 0.96, leading to an impressive F1-score of 0.97. In the urban class, precision is 0.70, with a recall of 0.77, resulting in an F1-score of 0.73. The water class showcases remarkable metrics, boasting a precision of 0.98, a recall of 0.98, and an outstanding F1-score of 0.98, emphasizing the overall excellence of the classification process.

Figure 4, which illustrates the classification of all four land use classes in testing area 1: Figure 4(a) high resolution satellite image and Figure 4(b) landcover map, shows that machine learning, utilizing Sentinel-1 time-series data polarization (Figures 4(c) to (k), is excellent in classifying land use and land cover types, especially for the water class. However, the second-best classification performance is observed in the classification of the rice class. This method can classify rice cultivation areas more accurately compared to the other classes, namely the agricultural/forest class, forest class, and urban class. It is apparent that employing random forest, XGBoost, and LightGBM methods in machine learning contributes to proficient classification of rice cultivation areas. In particular, LightGBM demonstrated superior performance in classifying rice cultivation areas with fewer classification errors, while random forest and XGBoost exhibited some errors in the classification of other classes. Upon closer examination, it is evident that VH+VV polarization enhances data classification efficiency to a greater extent compared to using VV or VH polarization alone. This enhanced diversity in data dimensions is particularly beneficial for the accurate classification of rice cultivation areas. However, the classification of agricultural/forest and urban areas remains a challenge for machine learning when compared Figure 5(a) high resolution satellite image and Figure 5(b) landcover map. As evidenced in Figures 5(c)-(k) showing testing area 2, some urban areas are misidentified as agricultural or forest areas. Despite this, using VH+VV polarization data reduces the classification error between these land cover types, underscoring the value of this data for increasing accuracy as shown in Figures 5(e), (h), and (k).

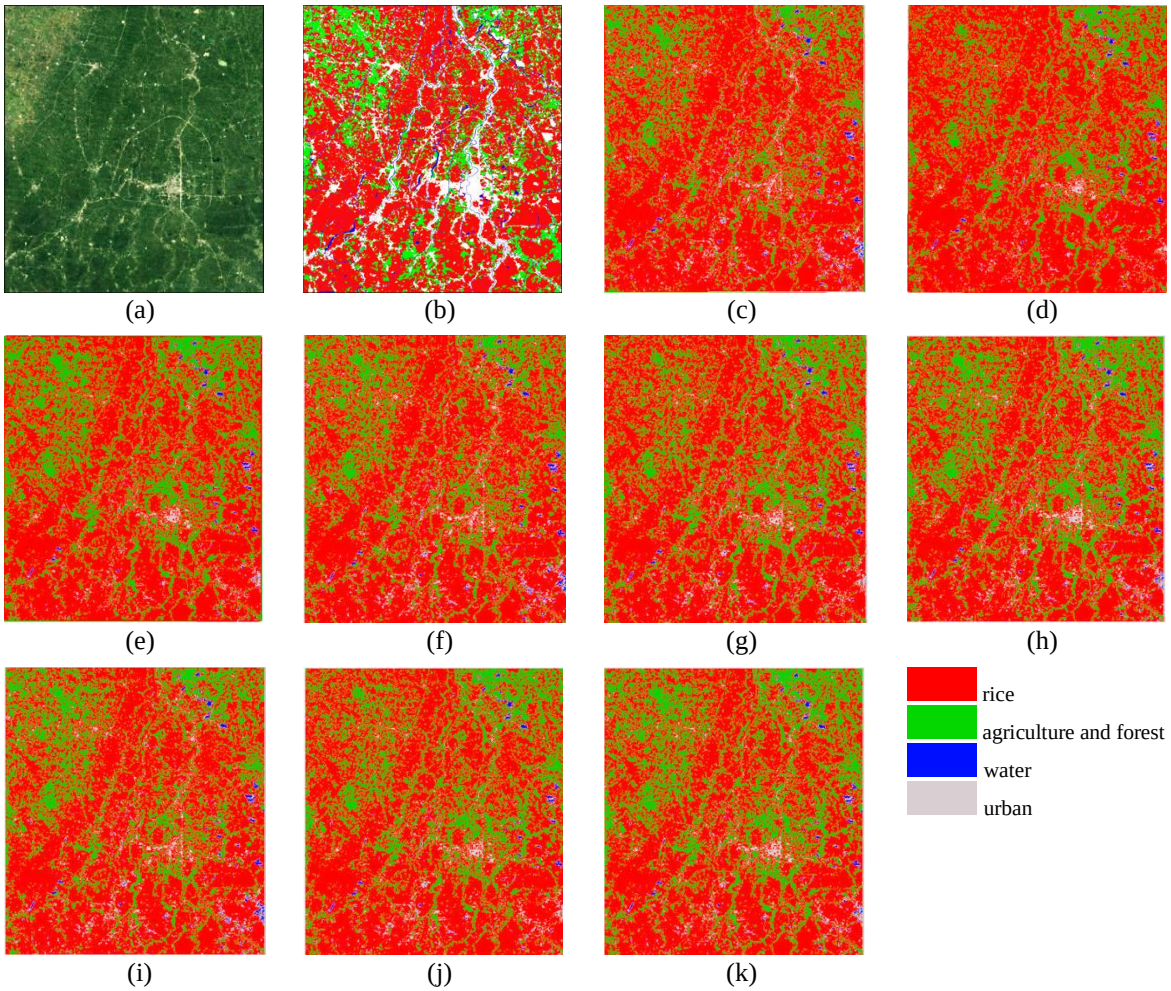

Figure 4. Rice classification results of machine learning algorithms applied to the testing area 1: (a) RGB images showing the landscape features, (b) reference map of land cover types, (c) VH polarization with RF algorithm, (d) VV polarization with RF algorithm, (e) VH and VV polarizations with RF algorithm, (f) VH polarization with XGBoost algorithm, (g) VV polarization with XGBoost algorithm, (h) VH and VV polarizations with XGBoost algorithm, (i) VH polarization with LightGBM algorithm, (j) VV polarization with LightGBM algorithm, and (k) VH and VV polarizations with LightGBM algorithm

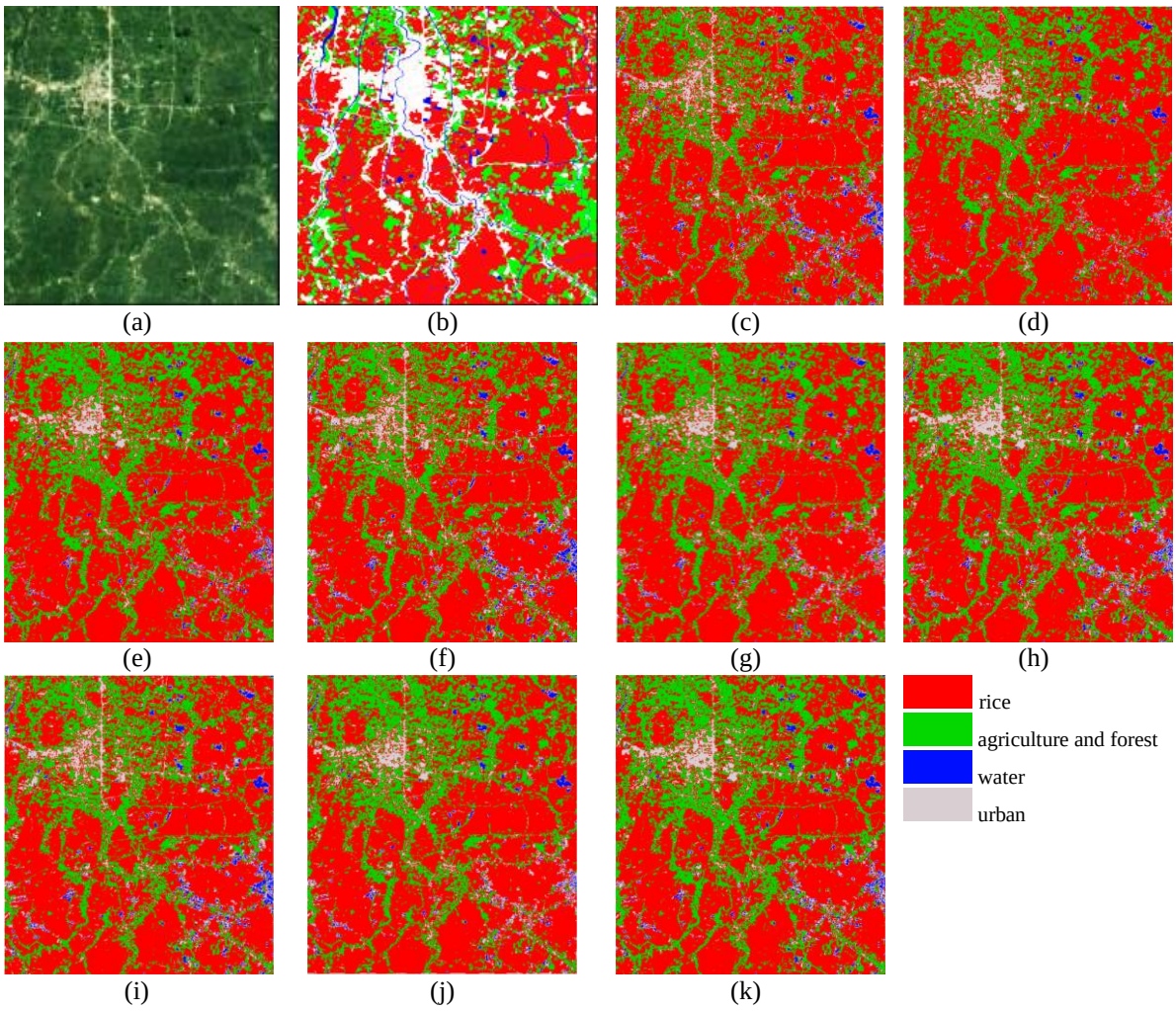

Figure 5. Rice classification results of machine learning algorithms applied to the testing area 2: (a) RGB images showing the landscape features, (b) reference map of land cover types, (c) VH polarization with RF algorithm, (d) VV polarization with RF algorithm, (e) VH and VV polarizations with RF algorithm, (f) VH polarization with XGBoost algorithm, (g) VV polarization with XGBoost algorithm, (h) VH and VV polarizations with XGBoost algorithm, (i) VH polarization with LightGBM algorithm, (j) VV polarization with LightGBM algorithm, and (k) VH and VV polarizations with LightGBM algorithm

5. DISCUSSION

This research presents a comprehensive analysis of rice crop classification using Sentinel-1 SAR time-series data with different polarization modes, leveraging machine learning algorithms. LightGBM, XGBoost, and random forest algorithms were employed to assess the performance of rice crop classification. This research found that fine-tuning hyperparameters and using time-series data polarization, specifically combining VV and VH polarizations, significantly enhanced the classification performance of all three machine learning algorithms. LightGBM, when optimized with hyperparameters (n_estimators: 820, max_depth: 10, learning_rate: 0.01), achieved the highest overall accuracy and Kappa coefficient among the tested models. This combination outperformed the single polarization scenarios (VV and VH) significantly, aligning with the results of Mansaray *et al.* [34], who demonstrated that combining VH and VV polarizations improves mapping accuracy for paddy rice fields.

LightGBM with VV+VH polarization achieved an overall accuracy of 91.64%, compared to 89.11% with VV polarization and 85.46% with VH polarization. XGBoost and random forest showed similar trends, with VV+VH polarization consistently yielding higher accuracy and Kappa coefficients. This underscores the effectiveness of combining multiple polarizations to capture comprehensive features that enhance the differentiation between various land cover types. The superior performance of LightGBM is also attributed to its ability to handle large datasets efficiently and extract significant patterns from multi-dimensional feature spaces.

The comparison of machine learning algorithms demonstrates that LightGBM outperforms XGBoost and random forest across all performance metrics. It indicates its superior capability in handling large and complex datasets and providing robust predictions for rice classification. The enhanced performance of LightGBM can be credited to its advanced techniques such as GOSS and EFB, which optimize training speed and memory efficiency while maintaining high predictive accuracy. Additionally, the leaf-wise tree growth strategy used by LightGBM enables it to achieve faster convergence and higher accuracy by prioritizing splits with the most significant impact. However, the classification accuracy for the agriculture/forest class and urban classes was relatively lower due to their complex features and overlapping characteristics.

These results are consistent with the challenges highlighted by Mansaray *et al.* [34], where distinguishing between mixed land-use categories proved difficult. While the results achieved high precision, recall, and F1-scores for the rice class and water class, the agriculture/forest class and urban class exhibited more classification errors. These unexpected errors suggest the need for further refinement in data preprocessing, feature extraction, and algorithm tuning to improve classification accuracy for more complex land use categories. Incorporating additional spectral, temporal, and spatial features may enhance the model's ability to differentiate between similar classes. Furthermore, the classification results for each land use class, as shown in Table 4, indicate that LightGBM consistently provides the most accurate and precise classifications. Particularly, the VV+VH polarization data yields the most accurate rice field maps, with minimal misclassifications compared to VV and VH polarizations alone.

This combination leverages the complementary information provided by the VV and VH polarizations, capturing subtle variations in backscatter signals indicative of rice fields at different growth stages. Figures 4(e), (h), and (k) illustrates that the VV+VH polarization data enhances the classifier's ability to distinguish rice fields from other land use types, resulting in clearer and more distinct boundaries. The reference data confirms that the LightGBM classifier with VV+VH polarization matches the actual land use distribution, highlighting its superior performance in capturing the spatial patterns of rice cultivation areas. It produced maps with more accurate and distinct boundaries for rice fields compared to those generated by XGBoost and random forest. This performance can be attributed to LightGBM's ability to handle high-dimensional data and its robustness against noisy and incomplete data, making it particularly well-suited for complex remote sensing tasks. Despite this, some misclassifications between the agriculture/forest class, and urban class persist, underscoring the need for further refinement in distinguishing these complex categories.

In this particular area, our research focuses on the classification of rice crops using Sentinel-1 SAR time-series data with different polarization modes, enhanced by machine learning algorithms. We specifically employed LightGBM, XGBoost, and random forest to evaluate the performance of rice crop classification. Our findings revealed that fine-tuning hyperparameters and utilizing combined VV and VH polarizations significantly improved the classification accuracy for all three algorithms. LightGBM, when optimized with specific hyperparameters, achieved the highest overall accuracy and Kappa coefficient, demonstrating its superior ability to handle large datasets and extract significant patterns from multi-dimensional feature spaces. This combined VV+VH polarization approach yielded an overall accuracy of 91.64%, outperforming the single polarization scenarios. However, challenges remain in accurately classifying more complex land use types, indicating the need for further research. Future studies should explore the integration of additional data sources, such as multi-sensor data and increased temporal resolution, to enhance classification accuracy. Additionally, developing more sophisticated models to address the intricacies of complex land cover categories will be crucial for advancing the field of remote sensing and agricultural monitoring. Incorporating techniques such as deep learning, transfer learning, and ensemble methods may provide further improvements in classification performance. Moreover, conducting extensive field validation and cross-regional studies will help generalize the models to different geographical areas and diverse agricultural practices. This research lays the groundwork for future advancements in remote sensing-based agricultural monitoring, contributing to more effective and sustainable agricultural management practices globally.

6. CONCLUSION

This study demonstrates the effectiveness of using Sentinel-1 SAR time-series data polarization combined with advanced machine learning algorithms for rice area classification. The results show that this dual-polarization (VV+VH) approach significantly enhances classification accuracy compared to single polarization, and LightGBM outperforms other algorithms like XGBoost and random forest in terms of accuracy and robustness. It lays a strong foundation for more accurate and efficient agricultural monitoring and management. While the classification of rice fields was highly accurate, challenges remain with more complex land use classes such as agriculture/forest and urban areas which often exhibit overlapping and complex features. In the future, it should explore integrating additional data sources and advanced techniques

to address these challenges and further improve classification performance. This research provides a solid foundation for advancing remote sensing-based agricultural monitoring, contributing to more effective and sustainable agricultural management practices.

ACKNOWLEDGEMENTS

The authors would like to thank the Department of Geography, Faculty of Social Sciences, Srinakharinwirot University for their support. All authors would like to thank the Land Development Department in Thailand (https://www.ldd.go.th/) for Land use/Land cover data and the Office of Agricultural Economics (https://www.oae.go.th/) for rice field data. The reviewers and editors are deeply appreciated by all authors for their insightful, meticulous, and comprehensive feedback and recommendations on how to make the work better.

REFERENCES

[1] "Cereals; rice, broken exports by country |2021," [Online]. Available: https://wits.worldbank.org/trade/comtrade/en/country/ALL/year/2021/tradeflow/Exports/partner/WLD/product/100640.(Accessed: Oct. 07, 2023).
[2] J. J, "Thailand rice: recent dry conditions after a promising start; optimism still remains for this crop season," Commodity Intelligence Report, 2021. [Online]. Available: https://ipad.fas.usda.gov/. (Accessed: Oct. 07, 2023).
[3] I. P. de Lima, R. G. Jorge, and J. L. M. P. de Lima, "Remote sensing monitoring of rice fields: towards assessing water saving irrigation management practices," *Frontiers in Remote Sensing*, vol. 2, 2021, doi: 10.3389/frsen.2021.762093.
[4] N. Kulo, "Benefits of the remote sensing data integration," *Conference: 1st Western Balkan Conference on GIS, Mine Surveying, Geodesy and Geomatic*, 2018.
[5] S. Han and J. P. Kerekes, "Overview of passive optical multispectral and hyperspectral image simulation techniques," *IEEE Journal of Selected Topics in Applied Earth Observations and Remote Sensing*, vol. 10, no. 11, pp. 4794–4804, Nov. 2017, doi: 10.1109/JSTARS.2017.2759240.
[6] W. M. Brown, "Synthetic aperture radar," *IEEE Transactions on Aerospace and Electronic Systems*, vol. AES-3, no. 2, pp. 217–229, Mar. 1967, doi: 10.1109/TAES.1967.5408745.
[7] C. Rossi and E. Erten, "Paddy-rice monitoring using TanDEM-X," *IEEE Transactions on Geoscience and Remote Sensing*, vol. 53, no. 2, pp. 900–910, Feb. 2015, doi: 10.1109/TGRS.2014.2330377.
[8] Y. Inoue, E. Sakaiya, and C. Wang, "Capability of C-band backscattering coefficients from high-resolution satellite SAR sensors to assess biophysical variables in paddy rice," *Remote Sensing of Environment*, vol. 140, pp. 257–266, Jan. 2014, doi: 10.1016/j.rse.2013.09.001.
[9] S. Yang, S. Shen, B. Li, T. Le Toan, and W. He, "Rice mapping and monitoring using ENVISAT ASAR data," *IEEE Geoscience and Remote Sensing Letters*, vol. 5, no. 1, pp. 108–112, Jan. 2008, doi: 10.1109/LGRS.2007.912089.
[10] L. Chang, Y.-T. Chen, J.-H. Wang, and Y.-L. Chang, "Rice-field mapping with Sentinel-1A SAR time-series data," *Remote Sensing*, vol. 13, no. 1, Jan. 2021, doi: 10.3390/rs13010103.
[11] H. Phan, T. Le Toan, and A. Bouvet, "Understanding dense time series of Sentinel-1 backscatter from rice fields: case study in a Province of the Mekong Delta, Vietnam," *Remote Sensing*, vol. 13, no. 5, Jan. 2021, doi: 10.3390/rs13050921.
[12] J. B. Chen, "Rice crop classification using Sentinel-1A SAR data in Central Taiwan," National Central University Taoyuan City, Taiwan, 2016.
[13] L. Mansaray, D. Zhang, Z. Zhou, and J. Huang, "Evaluating the potential of temporal Sentinel-1A data for paddy rice discrimination at local scales," *Remote Sensing Letters*, vol. 8, pp. 967–976, Oct. 2017, doi: 10.1080/2150704X.2017.1331472.
[14] D. B. Nguyen and W. Wagner, "European rice cropland mapping with Sentinel-1 data: the Mediterranean Region case study," *Water*, vol. 9, no. 6, Jun. 2017, doi: 10.3390/w9060392.
[15] K. Harfenmeister, D. Spengler, and C. Weltzien, "Analyzing temporal and spatial characteristics of crop parameters using Sentinel-1 backscatter data," *Remote Sensing*, vol. 11, no. 13, Jan. 2019, doi: 10.3390/rs11131569.
[16] H. Bazzi *et al.*, "Mapping paddy rice using Sentinel-1 SAR time series in Camargue, France," *Remote Sensing*, vol. 11, no. 7, Jan. 2019, doi: 10.3390/rs11070887.
[17] B. Janga, G. Asamani, Z. Sun, and N. Cristea, "A review of practical AI for remote sensing in Earth sciences," *Remote Sensing*, vol. 15, no. 16, p. 4112, Aug. 2023, doi: 10.3390/rs15164112.
[18] S. Talukdar *et al.*, "Land-use land-cover classification by machine learning classifiers for satellite observations—a review," *Remote Sensing*, vol. 12, no. 7, 2020, doi: 10.3390/rs12071135.
[19] S. Pokhariyal, N. R. Patel, and A. Govind, "Machine learning-driven remote sensing applications for agriculture in India—a systematic review," *Agronomy*, vol. 13, no. 9, 2023, doi: 10.3390/agronomy13092302.
[20] S. M. Khan *et al.*, "A systematic review of disaster management systems: approaches, challenges, and future directions," *Land*, vol. 12, no. 8, 2023, doi: 10.3390/land12081514.
[21] B. Sirmacek and R. Vinuesa, "Remote sensing and AI for building climate adaptation applications," *Results in Engineering*, vol. 15, p. 100524, Sep. 2022, doi: 10.1016/j.rineng.2022.100524.
[22] F. Li, T. Yigitcanlar, M. Nepal, K. Nguyen, and F. Dur, "Machine learning and remote sensing integration for leveraging urban sustainability: a review and framework," *Sustainable Cities and Society*, vol. 96, p. 104653, 2023, doi: 10.1016/j.scs.2023.104653.
[23] I. H. Sarker, "Deep learning: a comprehensive overview on techniques, taxonomy, applications and research directions," *SN Computer Science*, vol. 2, no. 6, p. 420, Nov. 2021, doi: 10.1007/s42979-021-00815-1.
[24] G. Ke *et al.*, "LightGBM: a highly efficient gradient boosting decision tree," in *Proceedings of the 31st International Conference on Neural Information Processing Systems*, in NIPS'17. Red Hook, NY, USA: Curran Associates Inc., Dec. 2017, pp. 3149–3157.
[25] M. Hajihosseinlou, A. Maghsoudi, and R. Ghezelbash, "A novel scheme for mapping of MVT-Type Pb–Zn prospectivity: LightGBM, a highly efficient gradient boosting decision tree machine learning algorithm," *Natural Resources Research*, vol. 32, Aug. 2023, doi: 10.1007/s11053-023-10249-6.
[26] "Summary of land use types Suphan Buri Province, year 2021," Land Development Department, [Online]. Available: http://www1.ldd.go.th/WEB_OLP/Lu_64/Lu64_C/SPB2564.htm. (Accessed: Oct. 15, 2023).

[27] "Thailand." [Online]. Available: https://www.fao.org/4/Y4347E/y4347e1o.htm. (Accessed: Oct. 06, 2024).
[28] P. Vincent, "Sentinel-1 product specification," *ESA*, 2020.
[29] F. Filipponi, "Sentinel-1 GRD preprocessing workflow," *Proceedings*, vol. 18, no. 1, 2019, doi: 10.3390/ECRS-3-06201.
[30] L. Breiman, "Random forests," *Machine Learning*, vol. 45, no. 1, pp. 5–32, Oct. 2001, doi: 10.1023/A:1010933404324.
[31] T. Chen and C. Guestrin, "XGBoost: a scalable tree boosting system," in *Proceedings of the 22nd ACM SIGKDD International Conference on Knowledge Discovery and Data Mining*, in KDD '16. New York, NY, USA: Association for Computing Machinery, Aug. 2016, pp. 785–794, doi: 10.1145/2939672.2939785.
[32] G. Banko, "A review of assessing the accuracy of classifications of remotely sensed data and of methods including remote sensing data in forest inventory," International Institute for Applied Systems Analysis Interim Report, 1998.
[33] Y. Sasaki, "The truth of the F-measure," *Teach Tutor Mater*, Jan. 2007.
[34] L. R. Mansaray, V. T. S. Kabba, L. Zhang, and H. A. Bebeley, "Optimal multi-temporal Sentinel-1A SAR imagery for paddy rice field discrimination; a recommendation for operational mapping initiatives," *Remote Sensing Applications: Society and Environment*, vol. 22, p. 100533, Apr. 2021, doi: 10.1016/j.rsase.2021.100533.

BIOGRAPHIES OF AUTHORS

Attawut Nardkulpat holds a B.Sc. in Geography (2013) and an M.Sc. in Geoinformatics (2017), both from Burapha University, Thailand. Currently, he is pursuing a Ph.D. in Geoinformatics at Srinakharinwirot University, Bangkok, while also working as a remote sensing data scientist at THAICOM PLC. His research focuses on applying advanced technologies like GIS, remote sensing, deep learning, machine learning, and natural language processing to solve geographical challenges. He can be contacted at email: attawut.nardkulpat@g.swu.ac.th.

Wuttichai Boonpook has a diverse educational background with degrees in Geography (B.A., Thammasat University, 2009), International Business (B.B.A, Ramkhamhaeng University, 2009), spatial information systems engineering (M.Sc., Chulalongkorn University, 2013), and Traffic and Transportation Engineering (D.Eng., Beihang University, China, 2019). He currently lectures in the Department of Geography at Srinakharinwirot University, Bangkok. His research explores the applications of GIS and remote sensing, with a particular focus on deep learning for semantic segmentation of remote sensing data and UAV-based remote sensing. He can be contacted at email: wuttichaib@g.swu.ac.th.

Asamaporn Sitthi graduated from Chulalongkorn University (Bangkok, Thailand) in 2008 with a B.Sc. in Imaging Science and Printing Technology. She then earned her M.Sc. (2010) and Ph.D. (2016) in Remote Sensing and Geographic Information Systems from the Asian Institute of Technology (Thailand). Currently, she is a lecturer in the Department of Geography, Faculty of Social Science, at Srinakharinwirot University in Bangkok. Her research interests include remote sensing applications, image processing techniques for remote sensing data, geosocial sensing applications, and WebGIS. She can be contacted at email: asamaporn@g.swu.ac.th.

Yumin Tan earned her B.Sc. in Surveying from Guilin University of Technology (Guangxi, China) in 1998. She then received her M.Sc. in Geodesy from Tsinghua University (Beijing, China) in 2001, and her Ph.D. in GIS from the Chinese Academy of Science (Beijing, China) in 2004. Currently, she serves as a Professor of Transportation Engineering and Dean of the Department of Civil Engineering. Her research focuses on intelligent remote sensing data analysis, UAV remote sensing, and trust evaluation of remote sensing products. She can be contacted at email: tanym@buaa.edu.cn.